JOURNAL OF APPLIED PHYSICS **114**, 154516 (2013)

Lower limits to metal-semiconductor contact resistance: Theoretical models and experimental data

Ashish Baraskar,[1,a)] A. C. Gossard,[2] and Mark J. W. Rodwell[2]
[1]*GLOBALFOUNDRIES, Yorktown Heights, New York 10598, USA*
[2]*Departments of Materials and ECE, University of California, Santa Barbara, California 93106, USA*

(Received 7 August 2013; accepted 3 October 2013; published online 21 October 2013)

We calculate the minimum feasible contact resistivity to n-type and p-type $In_{0.53}Ga_{0.47}As$, InAs, GaAs, GaSb, InP, and InSb. The calculations consider image force lowering and assume either parabolic or non-parabolic energy dispersion in the semiconductor; their results are compared with recent experimental data. Among significant results, the measured contact resistivity to n-$In_{0.53}Ga_{0.47}As$ at a carrier concentration of $5 \times 10^{19}\,\mathrm{cm}^{-3}$ is only 2.3:1 higher than that calculated assuming a 0.2 eV barrier potential, and the measured contact resistivity is only 9.0:1 larger than the Landauer quantum conductivity limit at this carrier concentration. These results indicate that, with the surface preparation procedures presently employed, surface contamination does not markedly increase the interface resistance, and that the transmission coefficient for carriers crossing the interface exceeds 10%. *© 2013 AIP Publishing LLC*. [http://dx.doi.org/10.1063/1.4826205]

I. INTRODUCTION

The continued improvement of ohmic metal-semiconductor contacts is critical both to the development of nm transistors for VLSI and to the development of THz transistors for mm-wave wireless systems. In the extension by scaling of III–V bipolar and field-effect transistor bandwidths to 3–4 THz cutoff frequencies, ohmic contacts of below $\sim 10^{-8}\,\Omega - \mathrm{cm}^2$ resistivity are required.[1,2] In VLSI, as MOSFET source and drain contact areas are reduced to accommodate source-drain contact pitches of ∼50–100 nm, contacts of similarly low resistivity are required to permit high transistor on-state current. Ohmic contacts to group IV (Si, Ge) and III–V compound semiconductors have been extensively studied; results are summarized in Refs. 3 and 4. The primary factors determining contact resistivity are carrier concentration, semiconductor surface preparation and cleaning, and contact metal work function hence Schottky barrier height.[5–7] At a given carrier concentration in the semiconductor, there is lower limit below which the contact resistivity cannot be reduced. This lower limit results from the finite interface transmission probability, the finite carrier velocity, and the finite number of states available for carrier transport across the metal-semiconductor interface. Recently, Maassen *et al.*[8] calculated the intrinsic lower limit for contact resistivity for InAs, $In_{0.53}Ga_{0.47}As$, GaSb, and Si using a full band ballistic quantum transport approach. The authors found that, for a given carrier concentration, the lower limit for the contact resistivity is almost independent of the semiconductor.

Here, we present calculations of contact resistivities for n-type and p-type $In_{0.53}Ga_{0.47}As$, InAs, GaAs, GaSb, InP, and InSb. To compare these calculations to experimental data, three cases are addressed. First, the contact resistivity is calculated in the (typical) case where carriers must tunnel through a Schottky barrier of significant thickness. To assess the degree to which tunneling probability contributes to the interface resistance, the contact resistivity is also calculated for the case where this barrier is absent, i.e., with a step change in the electron affinity between the metal and the semiconductor. In this case, which we refer to as a step barrier, although carriers need not tunnel through a barrier, the interface transmission probability remains less than unity because of the abrupt change at the interface of the carrier potential energy and carrier effective mass. Finally, we calculate the contact resistivity assuming unity for the interface transmission probability, i.e., the resistivity in the quantum conductivity limit.

By comparing experimental data to resistivities calculated including the finite Schottky barrier, we can estimate the degree to which contact resistivity has been increased by surface contamination or other imperfections at the interface. By comparing the Landauer quantum conductivity limit to the resistivities calculated including the finite Schottky barrier, we can infer the contribution of the Schottky barrier transmission probability to the contact resistance.

II. CURRENT DENSITY AND CONTACT RESISTIVITY CALCULATIONS

We first present the method used to calculate the transmission probability and contact resistivity of a metal-semiconductor interface assuming either parabolic or non-parabolic energy dispersion in the semiconductor.

Assuming conservation of carrier transverse momentum and total energy, the net current density across a metal-semiconductor junction is[9]

$$J = \frac{2q}{(2\pi)^3} \int_{k_{sx}=-\infty}^{k_{sx}=\infty} \int_{k_{sy}=-\infty}^{k_{sy}=\infty} \int_{k_{sz}=0}^{k_{sz}=\infty} v_{sz}(f_s - f_m) T_P \, dk_{sx} dk_{sy} dk_{sz}, \quad (1)$$

where z is the direction of current flow and the xy plane is the plane parallel to the interface, v_{sz} is the z component of the

a)Author to whom correspondence should be addressed. Electronic mail: ashish.baraskar@globalfoundries.com

 © 2013 AIP Publishing LLC

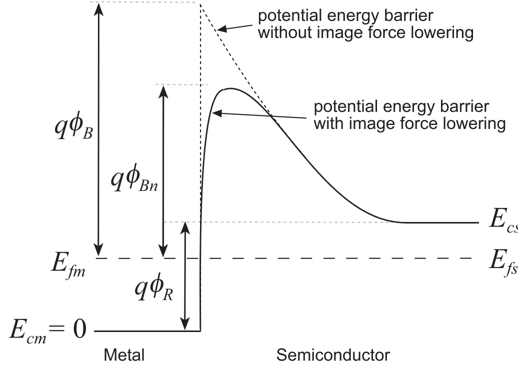

FIG. 1. Energy band diagram of the metal-semiconductor junction.

carrier group velocity in the semiconductor, $f_s = 1/(1+\exp(E-E_{fs})/kT)$ and $f_m = 1/(1+\exp(E-E_{fm})/kT)$ are the Fermi functions in the semiconductor and in the metal, $E = E(k_x, k_y, k_z)$ is the total carrier energy, E_{fs} and E_{fm} are the Fermi energies in the semiconductor and in the metal, k is the Boltzmann's constant, T is the temperature, $T_P = T_P(k_x, k_y, k_z)$ is the interface transmission probability, (k_{sx}, k_{sy}, k_{sz}) are the carrier wave vectors in the semiconductor in the (x, y, z) directions. Both $k_{sz}(z)$ and $v_{sz}(z)$ are functions of the depth (z) within the semiconductor; within Eq. (1), the quantities k_{sz} and v_{sz} are the asymptotic values taken at a large depth. To make analysis tractable, the free electron model and an idealized parabolic energy dispersion were assumed for the metal. The conduction band edge (E_{cm}) of the metal is taken, at 0 eV, as the reference energy (Fig. 1). As indicated in Fig. 1, $q\phi_R$ is the energy difference between the conduction band edge of the semiconductor (E_{cs}) and the conduction band edge of the metal (E_{cm}) i.e., $q\phi_R = E_{cs} - E_{cm}$. Also, $q\phi_B$ is the intrinsic barrier height and $q\phi_{Bn}$ is the barrier height at thermal equilibrium resulting due to image force lowering.

The contact resistivity, ρ_c, is defined as the inverse of the derivative of the current density by the voltage $V = (E_{fs} - E_{fm})/q$, as the voltage approaches zero

$$\frac{1}{\rho_c} = \left.\frac{dJ}{dV}\right|_{V=0}.$$

Hence, the contact resistivity is

$$\frac{1}{\rho_c} = \frac{2q^2}{(2\pi)^3 kT} \int_{k_{sx}=-\infty}^{k_{sx}=\infty} \int_{k_{sy}=-\infty}^{k_{sy}=\infty} \int_{k_{sz}=0}^{k_{sz}=\infty} \times \frac{v_{sz}\cdot \exp\left(\frac{E-E_{fs}}{kT}\right)}{\left(1+\exp\left(\frac{E-E_{fs}}{kT}\right)\right)^2} T_P dk_{sx}dk_{sy}dk_{sz}. \tag{2}$$

We now must consider separately the cases of parabolic and non-parabolic energy dispersion in the semiconductor.

Case I: For a semiconductor with parabolic energy dispersion, the total carrier energy is given by

$$E = q\phi_R + \frac{\hbar^2}{2m_s}(k_{sx}{}^2 + k_{sy}{}^2 + k_{sz}{}^2), \tag{3}$$

where m_s is the carrier effective mass in the semiconductor. In this case, the carrier group velocity is

$$v_{sz} = \frac{1}{\hbar}\frac{\partial E}{\partial k_{sz}} = \frac{\hbar k_{sz}}{m_s}, \tag{4}$$

from which we find,

$$\frac{1}{\rho_c} = \frac{2q^2\hbar}{(2\pi)^3 m_s kT} \int_{k_{st}=-\infty}^{k_{st}=\infty} \int_{k_{sz}=0}^{k_{sz}=\infty} \int_{\theta=0}^{\theta=2\pi} \times \frac{\exp\left(\frac{E-E_{fs}}{kT}\right)}{\left(1+\exp\left(\frac{E-E_{fs}}{kT}\right)\right)^2} T_P k_{st}dk_{st}k_{sz}dk_{sz}d\theta, \tag{5}$$

where $k_{st}{}^2 = k_{sx}{}^2 + k_{sy}{}^2$ and $dk_{sx}dk_{sy} = k_{st}dk_{st}d\theta$. From these, we find,

$$\frac{1}{\rho_c} = \frac{q^2\hbar}{2\pi^2 m_s kT} \int_{k_{st}=-\infty}^{k_{st}=\infty} \int_{k_{sz}=0}^{k_{sz}=\infty} \frac{\exp\left(\frac{E-E_{fs}}{kT}\right)}{\left(1+\exp\left(\frac{E-E_{fs}}{kT}\right)\right)^2} T_P k_{st}dk_{st}k_{sz}dk_{sz}. \tag{6}$$

Case II: The prior analysis assumed parabolic energy dispersion in the semiconductor, i.e., a quadratic variation of energy with momentum. The energy-momentum relationship is better approximated by a fourth-order (non-parabolic) dispersion relationship[10–12]

$$(E - q\phi_R)(1 + \alpha(E - q\phi_R)) = \frac{\hbar^2}{2m_s}(k_{st}{}^2 + k_{sz}{}^2), \tag{7}$$

where α is the non-parabolicity factor. From this, we find,

$$E = q\phi_R + \frac{1}{2\alpha}\left(\sqrt{1 + \frac{2\alpha\hbar^2(k_{st}{}^2 + k_{sz}{}^2)}{m_s}} - 1\right). \tag{8}$$

The group velocity is then,

$$v_{sz} = \frac{1}{\hbar}\frac{\partial E}{\partial k_{sz}} = \frac{\hbar k_{sz}}{m_s\sqrt{1 + \frac{2\alpha\hbar^2(k_{st}{}^2 + k_{sz}{}^2)}{m_s}}}. \tag{9}$$

From this, we find the contact resistivity,

$$\frac{1}{\rho_c} = \frac{q^2\hbar}{2\pi^2 m_s kT} \int_{k_{sx}=-\infty}^{k_{sx}=\infty} \int_{k_{sy}=-\infty}^{k_{sy}=\infty} \frac{v_{sz}}{\sqrt{1 + \frac{2\alpha\hbar^2(k_{st}{}^2 + k_{sz}{}^2)}{m_s}}} \times \frac{\exp\left(\frac{E-E_{fs}}{kT}\right)}{\left(1+\exp\left(\frac{E-E_{fs}}{kT}\right)\right)^2} T_P k_{st}dk_{st}k_{sz}dk_{sz}. \tag{10}$$

To evaluate these expressions to determine contact resistivity, the interface transmission probability must be calculated as a function of (k_x, k_y, k_z). This is shown next.

A. Calculation of the barrier transmission probability (T_P)

In prior work,[13] the Wentzel-Kramers-Brillouin (WKB) approximation has been used to calculate the transmission probability, T_P, across the metal-semiconductor interface. The WKB approximation breaks down at the regions close to the maximum of the potential energy barrier. The WKB approximation also neglects the quantum mechanical reflection arising from the abrupt change in electron affinity and carrier effective mass at the interface, an effect which becomes important for low-resistivity contacts having low Schottky barrier energy and highly degenerate carrier concentration in the semiconductor. Here, we present a more exact calculation of the transmission probability, a calculation which includes this interface reflection, and remains valid for carrier incident energy above the peak of the potential barrier.

To calculate the transmission probability, the potential energy is first calculated as a function of position. Image force barrier lowering is included in the calculation, but band gap narrowing due to highly degenerate carrier concentration was neglected. This computed potential profile is then approximated as a set of regions, each having a constant field, using the following procedure. First, the position $z = i$ of maximum field is identified (Fig. 2(a)), and the potential is then approximated as linear (constant field), with the modeled potential set equal to the exact computed potential at the point $z = i$. This constant field region extends over the interval $d_1 < z < d_2$; outside this region, the potential is modeled as constant potentials, either that of the barrier peak or that of the bulk semiconductor.

The barrier is thus separated into four adjacent constant-field regions. Within each region, Schrodinger's equation is solved using Airy functions. Within the region $0 < z < d_1$, an infinitesimal potential gradient $\delta q\phi_{Bn}$ is introduced (Fig. 2(b)) to facilitate the use of Airy functions. The Airy function solutions are valid in all the energy ranges,[14] i.e., $q\phi_R < E < \infty$ making the calculations less cumbersome. If a barrier with constant potential energy was chosen for this region ($0 < z < d_1$), it would require solutions of Schrodinger equations for $q\phi_R < E < q\phi_{Bn}$, $E = q\phi_{Bn}$, and $E > q\phi_{Bn}$ making the calculations tedious.

First, we calculate the transmission probability for a semiconductor with parabolic energy dispersion. For the barrier shown in Fig. 2(b), the potential energy for various regions is approximated by

$$V_1(z) = 0, \quad z \le 0, \tag{11}$$

$$V_2(z) = \phi_m - \delta\phi_{Bn} + s_1 z, \ 0 \le z \le d_1, \tag{12}$$

$$V_3(z) = \phi_m + \frac{\phi_m - \phi_R}{d_2 - d_1} d_1 - s_2 z, \ d_1 \le z \le d_2, \tag{13}$$

$$V_4(z) = \phi_R, \quad z \ge d_2, \tag{14}$$

where $\phi_m = \phi_M + \phi_{Bn}$, $s_1 = \delta\phi_{Bn}/d_1$, and $s_2 = (\phi_m - \phi_R)(d_2 - d_1)^{-1}$.

The wave functions required for calculating the transmission probability, T_P, are obtained by solving the

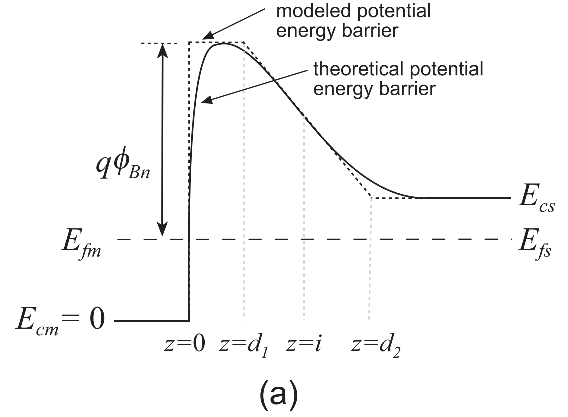

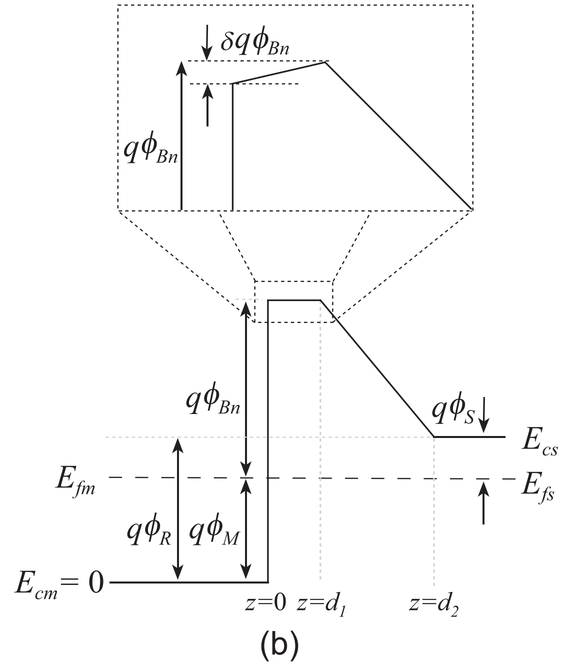

FIG. 2. (a) Schematic of the theoretical and modeled potential energy barrier. (b) Detailed schematic of the modeled potential energy barrier illustrating the approximation for the region $0 < z < d_1$.

time-independent Schrodinger equation, $(\hbar^2/2m_s)(\partial^2\psi/\partial z^2) + (E_z - V(z))\psi = 0$, for various constant-field regions of Fig. 2(b). The eigenfunction solutions of this equation for various regions are,

$$\psi_1(z) = \exp(ik_{mz}z) + R\exp(-ik_{mz}z), \quad z \le 0, \tag{15}$$

$$\psi_2(z) = CAi[\rho_1(qV_2(z) - E_z)] + DBi[\rho_1(qV_2(z) - E_z)], \quad 0 \le z \le d_1, \tag{16}$$

$$\psi_3(z) = FAi[\rho_2(qV_3(z) - E_z)] + GBi[\rho_2(qV_3(z) - E_z)], \quad d_1 \le z \le d_2, \tag{17}$$

$$\psi_4(z) = t\exp(ik_{sz}z), \quad z \ge d_2, \tag{18}$$

where $Ai(z)$ and $Bi(z)$ are the Airy functions,[15] R, C, D, F, G, and t are complex constants, $\rho_1 = (2m_s/\hbar^2 s_1^2)^{1/3}$, and $\rho_2 = (2m_s/\hbar^2 s_2^2)^{1/3}$.

Because the total energy, E, and the transverse wave vector k_t ($=k_{mt}=k_{st}$) does not change as carriers cross the interface,

$$E = E_{mt} + E_{mz} = q\phi_R + E_{st} + E_{sz}, \tag{19}$$

where $E_{mt} = \hbar^2 k_t^2/2m_m$ and $E_{mz} = \hbar^2 k_{mz}^2/2m_m$ are the components of the carrier kinetic energy in the metal associated with motion parallel to and perpendicular to the metal-semiconductor interface, and m_m is the carrier effective mass in the metal. Similarly, $E_{st} = \hbar^2 k_t{}^2/2m_s$ and $E_{sz} = \hbar^2 k_{sz}^2/2m_s$ are the components of the kinetic energy of the carrier in semiconductor parallel and perpendicular to the metal-semiconductor interface. Note, again, that a parabolic energy dispersion relationship is assumed for the metal.

From the continuity of $\psi(z)$ and $m^{-1}\partial\psi(z)/\partial z$ (Ref. 16) at the interfaces $z=0$, $z=d_1$, and $z=d_2$, six equations are obtained from which the six unknown complex constants can be determined. Hence,

$$t = \frac{2}{a_{10}(A_{10} + a_1 A_{10p}) + a_{11}(B_{10} + a_1 B_{10p})}. \tag{20}$$

The parameters $a_{10}, A_{10}, a_1, A_{10p}, a_{11}, B_{10}, a_1, B_{10p}$ are defined in Appendix A. The transmission probability is then given by

$$T_P = \frac{k_{sz}}{k_{mz}}\frac{m_m}{m_s}|t|^2. \tag{21}$$

Transmission probability was also calculated for a step barrier (Fig. 3). In this case, the electric field within the semiconductor is assumed to be zero. Although in this case, carriers crossing the interface must no longer tunnel through a Schottky potential barrier (Fig. 2), we will find that the transmission probability remains significantly below unity because of the abrupt change in carrier effective mass and kinetic energy. Comparison of the Schottky barrier, step barrier, and 100% transmission (quantum conductivity) cases permits us to infer the relative contributions of barrier tunneling and of mass and energy changes to the resistance. The interface transmission probability for this case, derived in Appendix B, is

$$T_P = \frac{k_{sz}}{k_{mz}}\frac{m_m}{m_s}\left|\frac{2k_{mz}/m_m}{k_{mz}/m_m + k_{sz}/m_s}\right|^2. \tag{22}$$

Next, we discuss the case for a semiconductor with non-parabolic energy dispersion. As shown in Eqs. (16) and (17), the kinetic energy associated with motion in the z direction is required to calculate the transmission probability across the tunnel barrier. For a semiconductor with non-parabolic energy dispersion, the total energy is,[10–12]

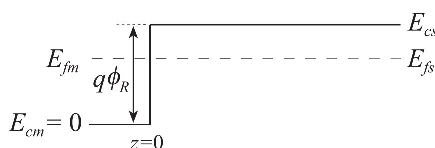

FIG. 3. Schematic of a step barrier.

$$E = q\phi_R + \frac{1}{2\alpha}\left(\sqrt{1 + \frac{2\alpha\hbar^2(k_t^2 + k_{sz}^2)}{m_s}} - 1\right). \tag{23}$$

Hence, for this case, we have calculated the interface transmission coefficient only for the case of the step barrier. The calculations are given in Appendix C; the transmission probability is

$$T_P = \frac{k_{sz}}{k_{mz}}\frac{m_m}{m_s^*}\left|\frac{2k_{mz}/m_m}{k_{mz}/m_m + k_{sz}/m_s C}\right|^2, \tag{24}$$

where m_s^* is the energy dependent conductivity mass in a non-parabolic semiconductor and is defined as,[11,12]

$$m_s^* = m_s(1 + 2\alpha(E - q\phi_R)). \tag{25}$$

B. Landauer contact resistivity

In the general relationship of Eq. (10), the contact resistivity is bounded below by the case of unity interface transmission probability, i.e., $T_P = 1$. In this case, the quantum conductivity or Landauer limit,[17] the contact resistivity for an isotropic single-band-minimum semiconductor is

$$\frac{1}{\rho_c} = (q^2/\hbar)(3/8\pi)^{2/3} n^{2/3}, \tag{26}$$

where n is the carrier concentration. Equation (26) is the Landauer limit for the Γ-valley-minimum III-V semiconductors. In contrast, for anisotropic semiconductors having g band minima, with carrier concentrations n_{si} and x, y, and z (transport) direction masses m_{xi}, m_{yi}, m_{zi} for the ith valley,

$$\frac{1}{\rho_c} = (q^2/\hbar)(3/8\pi)^{2/3} \cdot \sum_{i=1}^{g} (m_{xi}m_{yi}/m_{zi}^2)^{1/6} n_{si}^{2/3}. \tag{27}$$

For contacts to (100) Si, for four of the six filled Δ conduction-band valleys, $m_x = m_l$, $m_y = m_t$, and $m_z = m_t$, while for the remaining two Δ valleys, $m_x = m_y = m_t$ and $m_z = m_l$, where m_t and m_l are the Δ valley transverse and longitudinal effective masses. In this case, we find

$$\rho_c^{-1} = (q^2/\hbar)(3/8\pi)^{2/3}(n/6)^{2/3}(4(m_l/m_t)^{1/6} + 2(m_t/m_l)^{1/3}), \tag{28}$$

where n is the total carrier concentration.

III. EXPERIMENTAL DATA

The contact resistivities calculated by the methods described above were compared to the experimental data for contacts made to n-type and p-type $In_{0.53}Ga_{0.47}As$, InAs, GaAs, GaSb, and InP. We had earlier reported ultra low contact resistivities to n-InAs, n-$In_{0.53}Ga_{0.47}As$, and p-$In_{0.53}Ga_{0.47}As$.[18–20] The contact resistivities were $(0.6 \pm 0.4) \times 10^{-8}\,\Omega\,\text{cm}^2$, $(1.1 \pm 0.5) \times 10^{-8}\,\Omega\,\text{cm}^2$, and $(0.6 \pm 0.5) \times 10^{-8}\,\Omega\,\text{cm}^2$ for n-InAs, n-$In_{0.53}Ga_{0.47}As$, and p-$In_{0.53}Ga_{0.47}As$, respectively. In addition to these data, the experimental contact resistivity data

TABLE I. Band parameters of various III-V compound semiconductors.[60,61]

Parameter	InAs	$In_{0.53}Ga_{0.47}As$	GaAs	InP	GaSb	InSb
Band gap energy (eV)	0.36	0.74	1.42	1.344	0.726	0.17
Electron effective mass, m_s/m_o	0.023	0.041	0.063	0.08	0.041	0.014
Light hole effective mass, m_{lh}/m_o	0.026	0.052	0.082	0.12	0.05	0.015
Heavy hole effective mass, m_{hh}/m_o	0.41	0.45	0.51	0.6	0.4	0.43
Non-parabolicity, α (eV^{-1})	2.73	1.24	0.64	0.67	1.36	5.72

for n-type and p-type InAs, $In_{0.53}Ga_{0.47}As$, GaAs, GaSb, and InP were obtained from the literature.[6,7,21–59] To best of our knowledge, no experimental contact resistivity data has been reported for contacts made to n-type and p-type InSb.

IV. RESULTS AND DISCUSSION

A. Effect of non-parabolicity, metal Fermi energy, and carrier effective mass in the metal

In this section, we present the theoretical contact resistivities calculated using the equations obtained in Sec. II. The dependence of contact resistivity on three factors, non-parabolicity(α), metal Fermi energy (ϕ_M), and carrier effective mass in metal (m_m) is discussed. For brevity, only the results obtained for n-type InAs are presented. The parameters used for the calculations are listed in Table I.

Fig. 4 compares the calculated contact resistivities for parabolic and non-parabolic energy dispersion for n-type InAs. A step barrier (Fig. 3) and a metal Fermi energy $\phi_M = 11.4$ eV (corresponding to molybdenum (Mo)[62]) were assumed for the calculations. Resistivities lie slightly above Landauer limits because of interface quantum reflectivity; parabolic and non-parabolic bands show differing $(E_{fs} - E_c)$ and hence differing interface reflectivity. Further, at a given carrier concentration, Landauer contact resistivities are slightly lower in Si than in Γ-minima III-V semiconductors because of anisotropy and because of the multiple band minima.

To observe the effect of metal Fermi energy (ϕ_M) on contact resistivity, contact resistivities were calculated using $\phi_M = 5$ eV and $\phi_M = 10$ eV. The calculations were done for a step barrier (Fig. 3) and for a finite tunnel barrier (Fig. 2), assuming parabolic energy dispersion in the semiconductor.

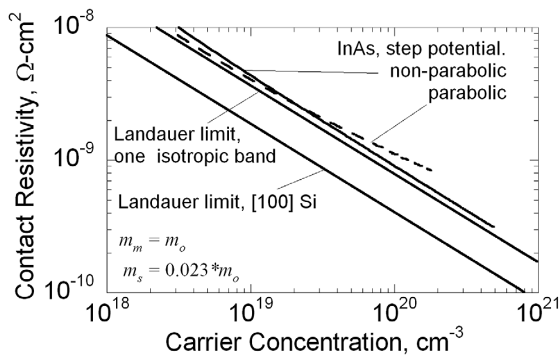

FIG. 4. Variation of contact resistivity with carrier concentration for parabolic and non-parabolic energy dispersion for n-type InAs. Landauer contact resistivity: for a single isotropic band and for (100) Si, and resistivity of InAs contact with a step barrier.

The results for the contact resistivities obtained for the step barrier are plotted in Fig. 5. It can be seen that the contact resistivities obtained for $\phi_M = 5$ eV lie below those obtained for $\phi_M = 10$ eV. Recalling that we here approximate the metal by the free-electron model, with the metal conduction-band energy taken as the reference energy at 0 eV, changing the metal Fermi energy corresponds to an assumed change in the metal's free electron concentration and changes the electron momentum (k-vector) at energies near the Fermi energy. Because of the wavefunction boundary conditions at the metal-semiconductor interface, changes in the metal Fermi energy, therefore, change the interface transmission coefficient. A similar trend was obtained for contact resistivities calculated for the finite tunnel barrier (not shown here).

The variation of contact resistivities of n-InAs with carrier concentration for different m_m is shown in Fig. 6. It can be seen that, as m_m increases, contact resistivity decreases. This could be because of the difference in the transmission probability for different carrier effective mass. To verify

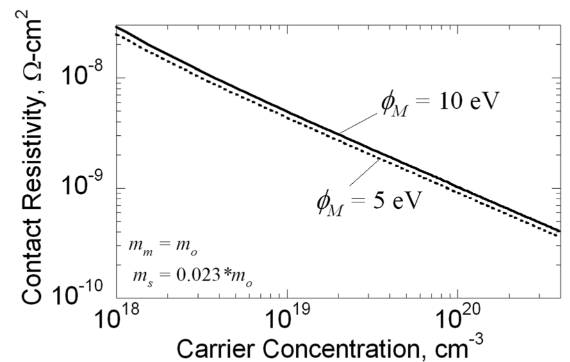

FIG. 5. Variation of contact resistivity with carrier concentration for $\phi_M = 5$ eV and $\phi_M = 10$ eV, for n-type InAs.

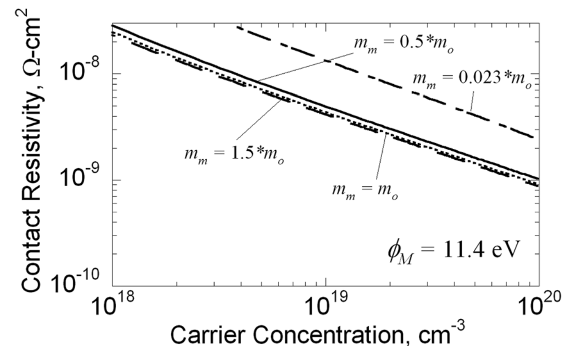

FIG. 6. Variation of contact resistivity with carrier concentration for various metal carrier effective mass (m_m) for n-type InAs.

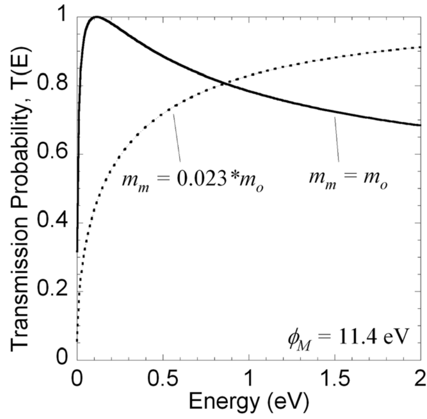

FIG. 7. Dependence of carrier transmission probability, T_P, on metal carrier effective mass (m_m) for n-type InAs.

this, T_P was calculated across a step barrier for two different m_m, i.e., $m_m = m_o$ and $m_m = 0.023m_o$ ($m_o = 9.1 \times 10^{-31}$ kg). The results are plotted in Fig. 7 which shows that T_P approaches unity at a lower energy for $m_m = m_o$, as compared to the case where $m_m = 0.023m_o$.[63] This difference in behavior of T_P with E could explain the higher contact resistivity obtained for $m_m = 0.023m_o$ as compared to that obtained for $m_m = m_o$.

B. Effect of Schottky barrier height (ϕ_B)

Contact resistivities were calculated for n-type and p-type $In_{0.53}Ga_{0.47}As$, InAs, GaAs, GaSb, InP, and InSb for different Schottky barrier heights, ϕ_B. As stated earlier, these calculations were done assuming parabolic energy dispersion in the semiconductors. For these calculations, $m_m = m_o$ and

FIG. 8. Calculated dependence (represented by lines) of contact resistivities (ρ_c) on bulk carrier concentration and Schottky barrier height (ϕ_B) for n-type/p-type $In_{0.53}Ga_{0.47}As$, InAs, GaAs, GaSb, InP, and InSb. Experimental data from Refs. 6, 7, 18–59 are also represented for comparison.

$\phi_M = 11.4$ eV (Fermi energy for Mo) were assumed. These calculations include image force lowering of the Schottky barrier at the metal semiconductor interface. The results are plotted in Figs. 8(a) to 8(l). Since the effective barrier height (ϕ_{Bn}) varies with the active carrier concentration due to image force lowering, only the value of ϕ_B is indicated in the figures. As expected, contact resistivities were found to depend strongly on ϕ_B. Experimental contact resistivities obtained from various references are also indicated in the figures. The contact resistivities obtained by *in situ* deposition of refractory metal contacts on n-type and p-type $In_{0.53}Ga_{0.47}As$, and n-type InAs[18–20] are shown in Figs. 8(a)–8(c), respectively. Even for contacts formed by *in situ* techniques, where interfaces are expected to have an oxide/-contaminant free metal-semiconductor interface, experimental resistivities of n-type contacts lie above theory given generally reported values of barrier potential. Measured contact resistivity to n-$In_{0.53}Ga_{0.47}As$ at $5 \times 10^{19}\,cm^{-3}$ carrier concentration is 2.3:1 higher than calculated assuming $\phi_B = 0.2$ eV, while measured contact resistivity to n-InAs at $10^{20}\,cm^{-3}$ carrier concentration is 1.9:1 higher than calculated assuming $\phi_B = 0$ eV. In contrast, measured contact resistivity to *p*-$In_{0.53}Ga_{0.47}As$ at $2.2 \times 10^{20}\,cm^{-3}$ carrier concentration correlates well with theory if $\phi_B = 0.6$ eV is assumed.

Calculations also show the degree to which the Schottky barrier increases contact resistivity. Computed contact resistivity for n-$In_{0.53}Ga_{0.47}As$ at $5 \times 10^{19}\,cm^{-3}$ carrier concentration and $\phi_B = 0.2$ eV is only 3.9:1 larger than the Landauer limit, while computed resistivity of n-InAs at $10^{20}\,cm^{-3}$ carrier concentration and $\phi_B = 0$ eV is only 3.6:1 larger than Landauer limit. For *p*-$In_{0.53}Ga_{0.47}As$ at $2.2 \times 10^{20}\,cm^{-3}$ carrier concentration and $\phi_B = 0.6$ eV, computed resistivity lies 13:1 above the Landauer limit; the tunneling probability remains low.

It must be noted that the experimental data include contact resistivities obtained for alloyed and non-alloyed contacts. In addition, the data points are plotted with respect to the bulk carrier concentration. Depending on the contact metal used, the carrier concentration near the contact region might differ from bulk carrier concentration. For example, Chen *et al.*[33] reported $\rho_c = 5 \times 10^{-7}\,\Omega\,cm^2$ and $3.8 \times 10^{-7}\,\Omega\,cm^2$ for Ge/Pd/Au and Ni/Ge/Au contacts, respectively, to n-GaAs (Fig. 8(e)). The carrier concentration in n-GaAs was $2.2 \times 10^{18}\,cm^{-3}$. They attributed the low ρ_c to the increased carrier concentration at the surface due to Ge diffusion in GaAs. Similarly, as shown in Fig. 8(j), Malina *et al.*[57] obtained extremely low contact resistivities for p-InP. Here,[57] Au-Be was used for contacting the semiconductor and $\rho_c = 2 \times 10^{-8}\,\Omega\,cm^2$ was obtained after annealing, for a carrier concentration of $(3–4) \times 10^{18}\,cm^{-3}$. The low ρ_c could be a result of increased carrier concentration at the interface due to Be dopant diffusion in InP.

V. CONCLUSIONS

We have computed the contact resistivity as a function of both carrier concentration and Schottky barrier potential for contacts to n-type and p-type $In_{0.53}Ga_{0.47}As$, InAs, GaAs, GaSb, InP, and InSb. Resistivities calculated for a finite tunnel barrier are compared to the case of 100% interface transmission probability, i.e., the quantum conductivity limit. These results are compared to experimentally measured contact resistivities, including the data for contacts using refractory contact metals deposited *in situ* on the semiconductor surface immediately after semiconductor growth and without breaking vacuum. Such *in situ* refractory contacts avoid both significant metal penetration into the semiconductor and significant interface contamination via exposure to the atmosphere.

Experimentally measured contact resistivities for heavily doped n-type $In_{0.53}Ga_{0.47}As$ and n-type InAs lie within ∼4:1 of the calculated resistivities, while measured contact resistivities for heavily doped p-type $In_{0.53}Ga_{0.47}As$ agree with theory to within experimental variation. Particularly for the case of n-type $In_{0.53}Ga_{0.47}As$ and InAs at carrier concentrations between $5 \times 10^{19}\,cm^{-3}$ and $10^{20}\,cm^{-3}$, where the Schottky barriers energies (∼0.2 eV) and Schottky barriers widths (∼0.5–1.5 nm) are both small, the interface transmission probability is high, with computed contact resistivities lying within a factor of four of the quantum transport limit. In this limit, contact resistivity is only further improved by increased carrier concentration, with resistivity varying as the inverse of the (2/3)rd power of carrier concentration. For p-type $In_{0.53}Ga_{0.47}As$, even at a carrier concentration of $10^{20}\,cm^{-3}$, the barrier tunneling probability remains low, and increased carrier concentration should result in further rapid decreases in contact resistivity. Such low-resistance contacts have important applications in both high-frequency (THz) III-V transistors and in nm-contact-pitch transistors in VLSI.

ACKNOWLEDGMENTS

This work was supported by the ONR and by the DARPA THz Electronics Program. We would like to thank Sandeep Ponnuru for his assistance with MATLAB programming.

APPENDIX A: PARAMETERS USED FOR THE CALCULATION OF TRANSMISSION PROBABILITY FOR SEMICONDUCTOR WITH PARABOLIC ENERGY DISPERSION

$$A_{10} = Ai[\rho_1(\phi_m - d\phi_{Bn} - E_z)];\ dA_{10}/dz = A_{10p},$$

$$B_{10} = Bi[\rho_1(\phi_m - d\phi_{Bn} - E_z)];\ dB_{10}/dz = B_{10p},$$

$$A_{11} = Ai[\rho_1(\phi_m - E_z)];\ dA_{11}/dz = A_{11p},$$

$$B_{11} = Bi[\rho_1(\phi_m - E_z)];\ dB_{11}/dz = B_{11p},$$

$$A_{21} = Ai[\rho_2(\phi_m - E_z)];\ dA_{21}/dz = A_{21p},$$

$$B_{21} = Bi[\rho_2(\phi_m - E_z)];\ dB_{21}/dz = B_{21p},$$

$$A_{22} = Ai[\rho_2(\phi_R - E_z)];\ dA_{22}/dz = A_{22p},$$

$$B_{22} = Bi[\rho_2(\phi_R - E_z)];\ dB_{22}/dz = B_{22p},$$

$$a_1 = -\frac{i m_m \rho_1 s_1}{m_s k_{mz}},$$

$$a_2 = -\frac{\rho_2 s_2}{\rho_1 s_1},$$

$$a_3 = -\frac{i k_{sz}}{\rho_2 s_2},$$

$$a_4 = (a_2 A_{21p} A_{11} - A_{21} A_{11p})/W,$$

$$a_5 = (a_2 B_{21p} A_{11} - B_{21} A_{11p})/W,$$

$$a_6 = (A_{21} B_{11p} - a_2 A_{21p} B_{11})/W,$$

$$a_7 = (B_{21} B_{11p} - a_2 B_{21p} B_{11})/W,$$

$$a_8 = -\exp(i k_{sz} d_2)(A_{22p} - a_3 A_{22})/W,$$

$$a_9 = \exp(i k_{sz} d_2)(B_{22p} - a_3 B_{22})/W,$$

$$a_{10} = (a_6 a_9 + a_7 a_8),$$

$$a_{11} = (a_4 a_9 + a_5 a_8),$$

$W =$ Wronskian of Airy functions[15] $= A_{ij} B_{ijp} - B_{ij} A_{ijp} = 1/\pi$; $i, j = 1, 2$.

APPENDIX B: TRANSMISSION PROBABILITY FOR A STEP BARRIER (PARABOLIC ENERGY DISPERSION)

$$\psi_1(z) = \exp(i k_{mz} z) + A \exp(-i k_{mz} z), \quad z \le 0,$$

$$\psi_2(z) = B \exp(i k_{sz} z), \quad z \ge d.$$

At $z = 0$,

$$\psi_1(0) = \psi_2(0),$$

$$\frac{1}{m_m}\frac{d\psi_1(0)}{dz} = \frac{1}{m_s}\frac{d\psi_2(0)}{dz},$$

which yields,

$$B = \frac{2k_{mz}/m_m}{k_{mz}/m_m + k_{sz}/m_s},$$

where

$$k_{sz} = \left(\frac{2 m_s E_{sz}}{\hbar^2}\right)^{1/2},$$

$$k_{mz} = \left(\frac{2 m_m (E - E_{st}(m_s/m_m))}{\hbar^2}\right)^{1/2}.$$

The transmission probability is then given by,

$$T_P = \frac{k_{sz}}{k_{mz}}\frac{m_m}{m_s}\left|\frac{2k_{mz}/m_m}{k_{mz}/m_m + k_{sz}/m_s}\right|^2.$$

APPENDIX C: TRANSMISSION PROBABILITY FOR A STEP BARRIER (NON-PARABOLIC ENERGY DISPERSION)

$$\psi_1(z) = \exp(i k_{mz} z) + A \exp(-i k_{mz} z), \quad z \le 0,$$

$$\psi_2(z) = B \exp(i k_{sz} z), \quad z \ge d.$$

At $z = 0$,

$$\psi_1(0) = \psi_2(0),$$

$$\frac{1}{m_m}\frac{d\psi_1(0)}{dz} = \frac{1}{m_s^*}\frac{d\psi_2(0)}{dz},$$

which yields,

$$B = \frac{2k_{mz}/m_m}{k_{mz}/m_m + k_{sz}/m_s^*},$$

where

$$k_{sz} = \left(\frac{2 m_s E_{sz}}{\hbar^2}\right)^{1/2},$$

$$k_{mz} = \left(\frac{2 m_m}{\hbar^2}\left(q\phi_R + \frac{1}{2\alpha}\left(\frac{m_s^*}{m_s} - 1\right) - \frac{\hbar^2 k_{st}^2}{2 m_s}\right)\right)^{1/2}.$$

The transmission probability is then given by,

$$T_P = \frac{k_{sz}}{k_{mz}}\frac{m_m}{m_s^*}\left|\frac{2k_{mz}/m_m}{k_{mz}/m_m + k_{sz}/m_s^*}\right|^2.$$

[1] M. J. W. Rodwell, M. Le, and B. Brar, "A future of integrated electronics: Moving beyond Moore's law and off the roadmap," in *Proceedings of the IEEE*, Special Issue (2008), Vol. 96, p. 271.
[2] M. J. W. Rodwell, E. Lobisser, M. Wistey, V. Jain, A. Baraskar, E. Lind, J. Koo, Z. Griffith, J. Hacker, M. Urteaga, D. Mensa, R. Pierson, and B. Brar, in IEEE Compound Semiconductor IC Symposium, Monterey, CA, 12–14 October 2008.
[3] J. P. Gambino and E. G. Colgan, Mater. Chem. Phys. **52**, 99 (1998).
[4] T. V. Blank and Y. A. Goldberg, Semiconductors **41**, 1263 (2007).
[5] S. M. Sze and K. K. Ng, *Physics of Semiconductor Devices* (John Wiley and Sons, Inc., Hoboken, New Jersey, 2007).
[6] V. Jain, A. Baraskar, M. A. Wistey, U. Singisetti, Z. Griffith, E. Lobisser, B. J. Thibeault, A. C. Gossard, and M. J. W. Rodwell, in Proceedings of the International Conference on Indium Phosphide and Related Materials, Newport Beach, CA, 10–14 May 2009.
[7] E. F. Chor, D. Zhang, H. Gong, W. K. Chong, and S. Y. Ong, J. Appl. Phys. **87**, 2437 (2000).
[8] J. Maassen, C. Jeong, A. Baraskar, M. Rodwell, and M. Lundstrom, Appl. Phys. Lett. **102**, 111605 (2013).
[9] J. W. Conley, C. B. Duke, G. D. Mahan, and J. J. Tiemann, Phys. Rev. **150**, 466 (1966).
[10] E. M. Conwell and M. O. Vassel, Phys. Rev. **166**, 797 (1968).
[11] E. Kane, J. Phys. Chem. Solids **1**, 249 (1957).
[12] T. Grasser, Physica A **349**, 221 (2005).
[13] C. R. Crowell and V. L. Rideout, Solid-State Electron. **12**, 89 (1969).
[14] D. N. Christodoulides, A. G. Andreou, R. I. Joseph, and C. R. Westgate, Solid-State Electron. **28**, 821 (1985).
[15] M. Abramowitz and I. Stegun, *Handbook of Mathematical Functions* (Dover, New York, 1970).

[16]R. Eisberg and R. Resnick, *Quantum Physics* (John Wiley and Sons, New York, 1985).
[17]R. Landauer, IBM J. Res. Dev. **1**, 223 (1957).
[18]A. Baraskar, M. A. Wistey, V. Jain, U. Singisetti, G. Burek, B. Thibeault, Y. J. Lee, A. Gossard, and M. J. W. Rodwell, J. Vac. Sci. Technol. B **27**, 2036 (2009).
[19]A. Baraskar, V. Jain, M. A. Wistey, U. Singisetti, Y. J. Lee, B. J. Thibeault, A. C. Gossard, and M. J. W. Rodwell, in Proceedings of 22nd IEEE International Conference on Indium Phosphide and Related Materials, Kagawa, Japan, May 31-June 4, 2010.
[20]A. Baraskar, V. Jain, M. A. Wistey, B. J. Thibeault, A. Gossard, and M. J. W. Rodwell, in 16th International Conference on Molecular Beam Epitaxy, Berlin, Germany, 22–27 August 2010.
[21]Y. H. Yeh, J. T. Lai, and J. Y. Lee, Jpn. J. Appl. Phys. **35**, L1569 (1996).
[22]G. Stareev, H. Kijnzel, and G. Dortmann, J. Appl. Phys. **74**, 7344 (1993).
[23]J. C. Lin, S. Y. Yu, and S. E. Mohney, J. Appl. Phys. **114**, 044504 (2013).
[24]A. Katz, A. El-Roy, A. Feingold, M. Geva, N. Moriya, S. J. Pearton, E. Lane, T. Keel, and C. R. Abernathy, Appl. Phys. Lett. **62**, 2652 (1993).
[25]V. Jain, E. Lobisser, A. Baraskar, B. J. Thibeault, M. J. W. Rodwell, Z. Griffith, M. Urteaga, S. T. Bartsch, D. Loubychev, A. Snyder, Y. Wu, J. M. Fastenau, and W. K. Liu, in Device Research Conference, South Bend, IN, 21–23 June 2010.
[26]P. Jian, D. G. Ivey, R. Bruce, and G. Knight, J. Mater. Sci.: Mater. Electron. **7**, 77 (1996).
[27]Y. Shiraishi, N. Furuhata, and A. Okamoto, J. Appl. Phys. **76**, 5099 (1994).
[28]U. Singisetti, M. A. Wistey, J. D. Zimmerman, B. J. Thibeault, M. J. W. Rodwell, A. C. Gossard, and S. R. Bank, Appl. Phys. Lett. **93**, 183502 (2008).
[29]C. T. Lee, K. L. Jaw, and C. D. Tsai, Solid-State Electron. **42**, 871 (1998).
[30]A. Katz, S. N. G. Chu, B. E. Weir, W. Savin, D. W. Harris, W. C. Dautremont-Smith, T. Tanbun-Ek, and R. A. Logan, J. Vac. Sci. Technol. B **8**, 1125 (1990).
[31]E. M. Lysczek, J. A. Robinson, and S. E. Mohney, Mater. Sci. Eng. B **134**, 44 (2006).
[32]R. Stall, C. E. C. Wood, K. Board, and L. F. Eastman, Electron. Lett. **15**, 800 (1979).
[33]C. L. Chen, L. J. Mahoney, M. C. Finn, R. C. Brooks, A. Chu, and J. Mavroides, Appl. Phys. Lett. **48**, 535 (1986).
[34]L. C. Wang, X. Z. Wang, S. S. Lau, T. Sands, W. K. Chan, and T. F. Kuech, Appl. Phys. Lett. **56**, 2129 (1990).
[35]K. Shenai, IEEE Trans. Electron Devices **34**, 1642 (1987).
[36]M. O. Aboelfotoh, M. A. Borek, and J. Narayan, Appl. Phys. Lett. **75**, 3953 (1999).
[37]I. G. Akdogan and M. A. Parker, Electrochem. Solid-State Lett. **8**, G106 (2005).
[38]C. H. Wu, S. M. Liao, and K. C. Chang, Mater. Sci. Eng., B **117**, 205 (2005).
[39]G. Stareev, Appl. Phys. Lett. **62**, 2801 (1993).
[40]M. Yanagihara and A. Tamura, Electron. Lett. **32**, 1238 (1996).
[41]M. P. Patkar, T. P. Chin, J. M. Woodall, M. S. Lundstrom, and M. R. Melloch, Appl. Phys. Lett. **66**, 1412 (1995).
[42]H. Shimawaki, N. Furuhata, and K. Honjo, J. Appl. Phys. **69**, 7939 (1991).
[43]R. Bruce, D. Clark, and S. Eicher, J. Electron. Mater. **19**, 225 (1990).
[44]Z. C. Yang, P. H. Hao, and L. C. Wang, Electron. Lett. **32**, 2348 (1996).
[45]K. Ikossi, M. Goldenberg, and J. Mittereder, Solid-State Electron. **46**, 1627 (2002).
[46]R. K. Huang, C. A. Wang, C. T. Harris, M. K. Connors, and D. A. Shiau, J. Electron. Mater. **33**, 1406 (2004).
[47]J. A. Robinson and S. E. Mohney, J. Appl. Phys. **98**, 033703 (2005).
[48]A. G. Milnes, M. Ye, and M. Stam, Solid-State Electron. **37**, 37 (1994).
[49]E. Villemain, S. Gaillard, M. Rolland, and A. Joullie, Mater. Sci. Eng. **20**, 162 (1993).
[50]A. Vogt, A. Simon, J. Weber, H. L. Hartnagel, J. Schikora, V. Buschmann, and H. Fuess, Mater. Sci. Eng., B **66**, 199 (1999).
[51]T. Clausen, A. S. Pedersen, and O. Leistiko, Microelectron. Eng. **15**, 157 (1991).
[52]P. A. Leigh, R. M. Cox, and P. J. Dobson, Solid-State Electron. **37**, 1353 (1994).
[53]F. Ren, M. J. Antonell, C. R. Abernathy, S. J. Pearton, J. R. LaRoche, M. W. Cole, J. R. Lothian, and R. W. Gedridge, Appl. Phys. Lett. **74**, 1845 (1999).
[54]W. C. Huang, T. F. Lei, and C. L. Lee, J. Appl. Phys. **78**, 6108 (1995).
[55]W. O. Barnard, G. Myburg, F. D. Auret, J. H. Potgieter, P. Ressel, and E. Kuphal, Vacuum **46**, 893 (1995).
[56]F. Ren, S. J. Pearton, J. R. Lothian, S. N. G. Chu, W. K. Chu, R. G. Wilson, C. R. Abernathy, and S. S. Pei, Appl. Phys. Lett. **65**, 2165 (1994).
[57]V. Malina, L. Moro, V. Micheli, and I. Mojzes, Semicond. Sci. Technol. **11**, 1121 (1996).
[58]Kefeng Zhang, Hengjing Tang, Xiaoli Wu, Jintong Xu, Xue Li, and Haimei Gong, Proc. SPIE **6621**, 662118 (2008).
[59]M. H. Park, L. C. Wang, J. Y. Cheng, and C. J. Palmstrom, Appl. Phys. Lett. **70**, 99 (1997).
[60]M. Levinshtein, S. Rumyantsev, and M. Shur, *Handbook Series on Semiconductor Parameters* (World Scientific Publishing, Singapore, 1999), Vol. 2.
[61]M. Lundstrom, *Fundamentals of Carrier Transport* (Cambridge University Press, 2000).
[62]R. J. Iverson and L. Hodges, Phys. Rev. B **8**, 1429 (1973).
[63]A. Levi, *Applied Quantum Mechanics* (Cambridge University Press, 2003).